Carbon dioxide removal and soil reclamation using principles of enhanced rock weathering in an acidic Indian soil

Abir Dey, Chandra Saha[1], Debashis Mandal, Binoy Sarkar[2], MC Meena, BB Basak, Debarup Das, Pradarshak Sen[1], and Bijan Kumar Mondal

Indian Agricultural Research Institute, New Delhi, India
[1]Indian Institute of Soil Science, Bhopal, India
[2]University of South Australia, Adelaide, Australia
Corresponding author E-mail ID: abirdey21@gmail.com

Introduction

- Enhanced rock weathering (ERW) is one of the potential negative emission technologies (NET) that sequester atmospheric CO_2 through the dissolution of silicate minerals.
- It is also capable of ameliorating soil acidity through the production of carbonates and bicarbonates (Dietzen *et al.* 2018).
- $CaSiO_3$/ $MgSiO_3$ + $2CO_2$ + $3H_2O$ → Ca^{2+}/ Mg^{2+} + $2HCO_3^-$ + H_4SiO_4 (Beerling *et al.* 2020).

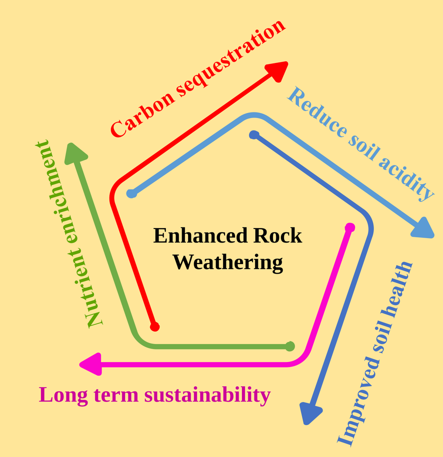

Objectives

- To assess the behavior of the basalt rock powder (BRD) in acid-aqueous solutions of different pH
- To evaluate the carbon emission in an acidic Inceptisol as impacted by the addition of BRD
- To study the effect of BRD on soil pH

Methodology

Table 1. Details of the treatment used to assess the behavior of BRD in acid-aqueous solutions

Treatment abbreviation	Treatment description
HCl_4	BRD + HCl solution, pH adjusted to 4.0
HCl_5	BRD + HCl solution, pH adjusted to 5.0
HCl_6	BRD + HCl solution, pH adjusted to 6.0
AA_4	BRD + Acetic acid solution, pH adjusted to 4.0
AA_5	BRD + Acetic acid solution, pH adjusted to 5.0
AA_6	BRD + Acetic acid solution, pH adjusted to 6.0

Table 2. Details of the treatment used for the incubation to study carbon emission from soil

Treatment abbreviation	Treatment description
Control	Soil
Lime	Soil + Lime (as per lime requirement of soil)
OM	Soil + Green manure + FYM
OM + $BRD_{2.5}$	Soil + Green manure + FYM + BRD@ 2.5 t ha^{-1}
OM + BRD_5	Soil + Green manure + FYM + BRD@ 5 t ha^{-1}
OM + BRD_{10}	Soil + Green manure + FYM + BRD@ 10 t ha^{-1}
OM + BRD_{25}	Soil + Green manure + FYM + BRD@ 25 t ha^{-1}
$BRD_{2.5}$	Soil + BRD@ 2.5 t ha^{-1}
BRD_5	Soil + BRD@ 5 t ha^{-1}
BRD_{10}	Soil + BRD@ 10 t ha^{-1}
BRD_{25}	Soil + BRD@ 25 t ha^{-1}

- **Experimental design:** Completely randomized design
- **Incubation experiment:** For 128 days at 25 ºC
- **Observation taken:** 1st, 2nd, 4th, 8th, 16th, 32nd, 64th and 128th day of incubation
- **Soil used:** sandy clay in texture with very low pH (4.01) from Assam, India

Results and discussion

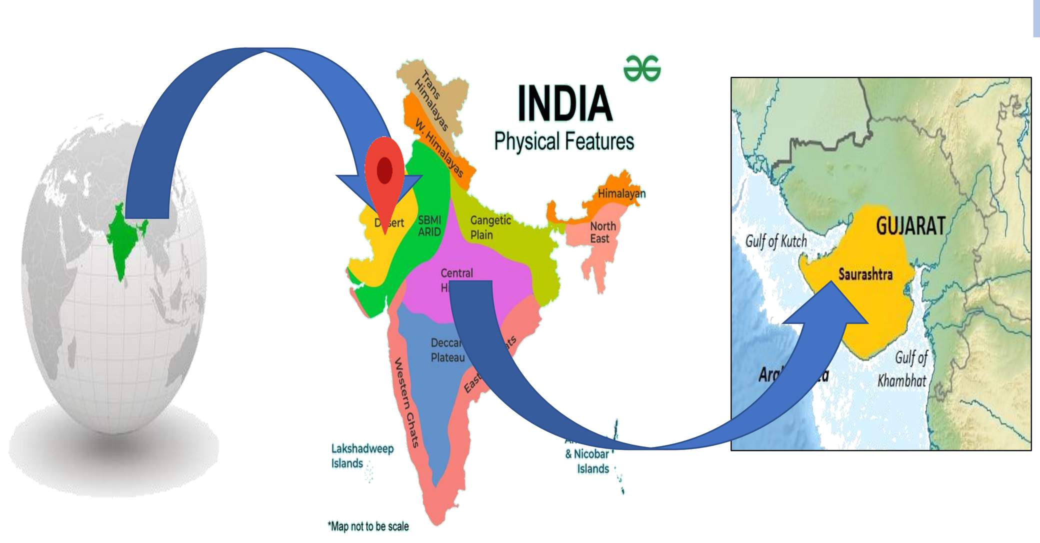

Basalt rock dust (BRD) used in these experiment, was collected from the Saurashtra region of Gujarat, India

Fig. 1. Relative proportion of silicate minerals in BRD

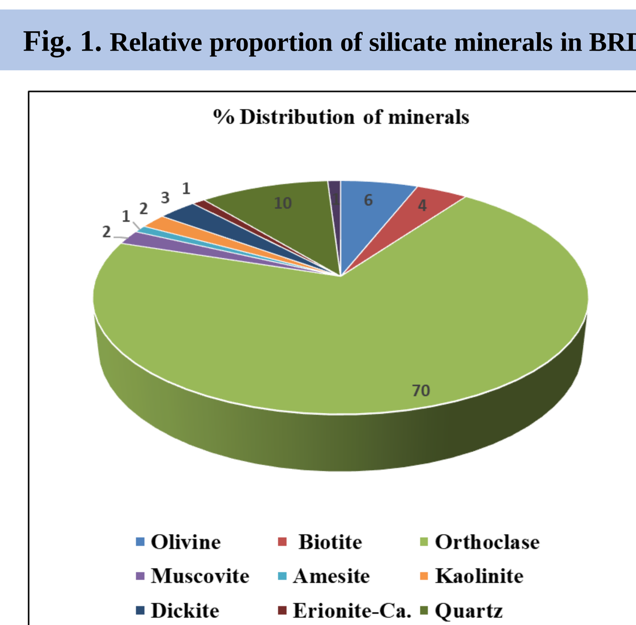

Fig. 2. Change in the pH of acid-aqueous Solutions (kept at different initial pH levels) due to BRD addition. Data represent the mean of 3 replicates. Error bar represents the standard error of estimation

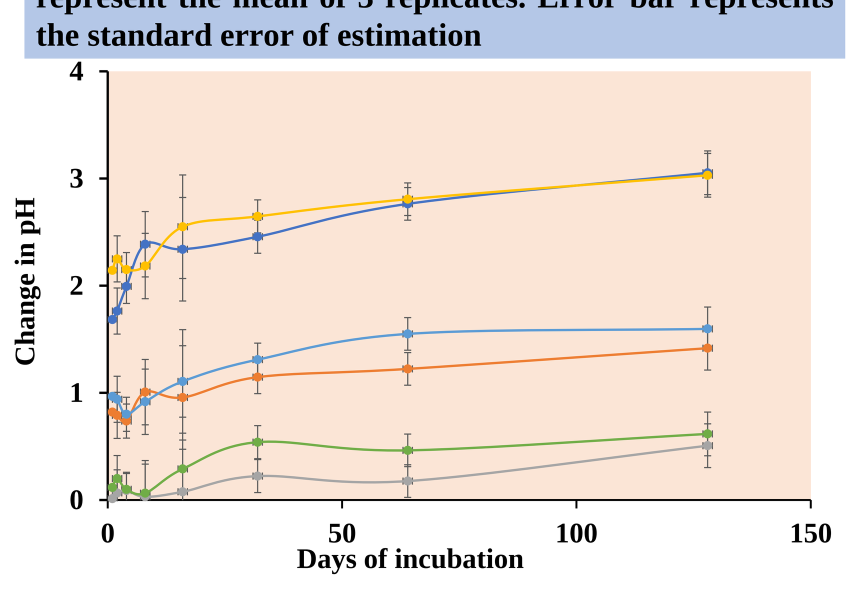

Fig. 3. Cumulative release of calcium and magnesium from the BRD in acid-aqueous solutions of different pH. Data represent the mean of 3 replicates. Error bar represents standard error of estimation

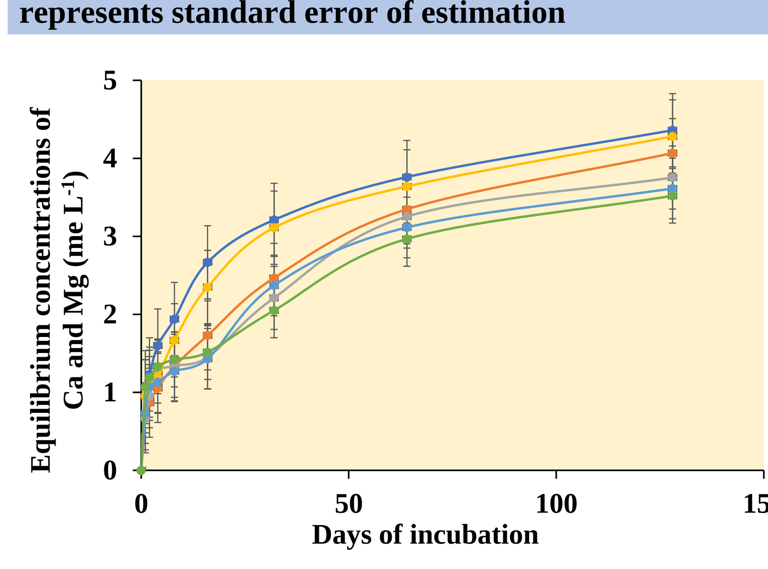

The highest increase in pH and basic cations due to BRD addition was observed in the treatment with the lowest initial pH (4.0)

Fig. 4. The cumulative carbon emissions from the soil treated with lime, organic matter and the rock mineral powder at 25 °C. The error bar represents LSD (p<0.05

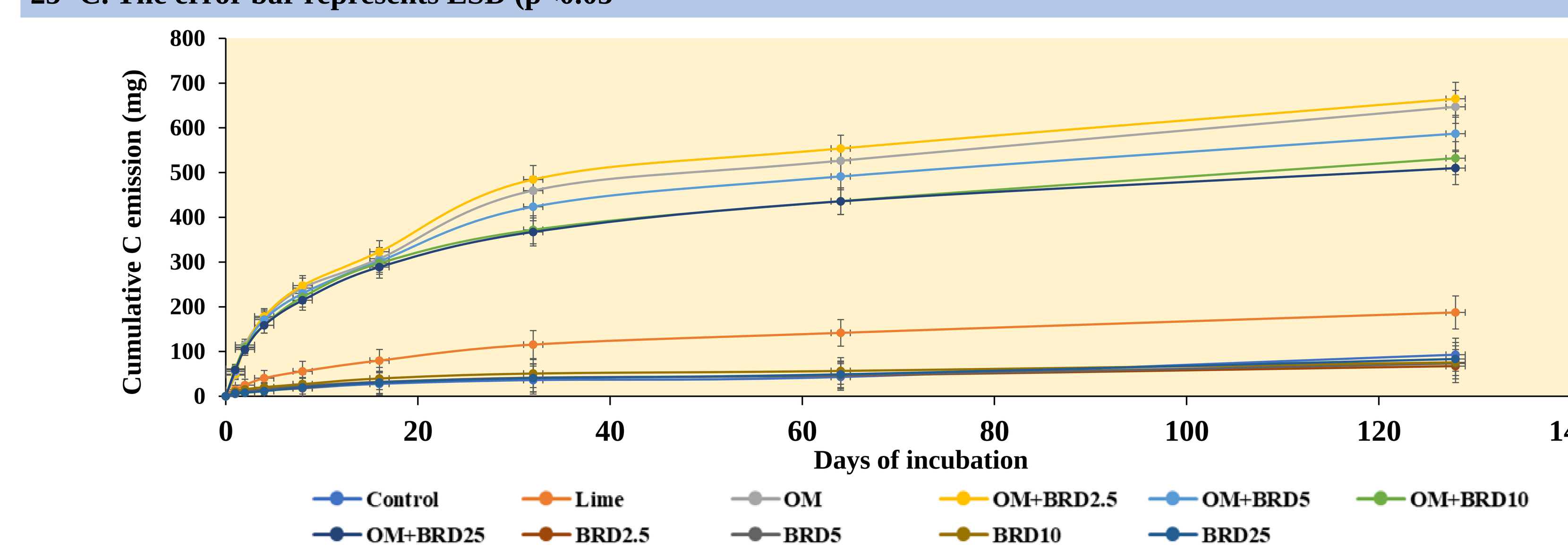

At the end of the incubation, the Ct followed the decreasing order: OM + RMP2.5 = OM > OM + RMP5 > OM + RMP10 = OM + RMP25 > Lime > RMP2.5 = RMP5 = RMP10 = RMP25 = control.

Fig. 5. The net cumulative carbon emission from the soil treated with lime, organic matter, and BRD. Data represent the mean of 3 replicates and error bar represent LSD at 5% level of significance. Different letters denote significant differences at p ≤ 0.05

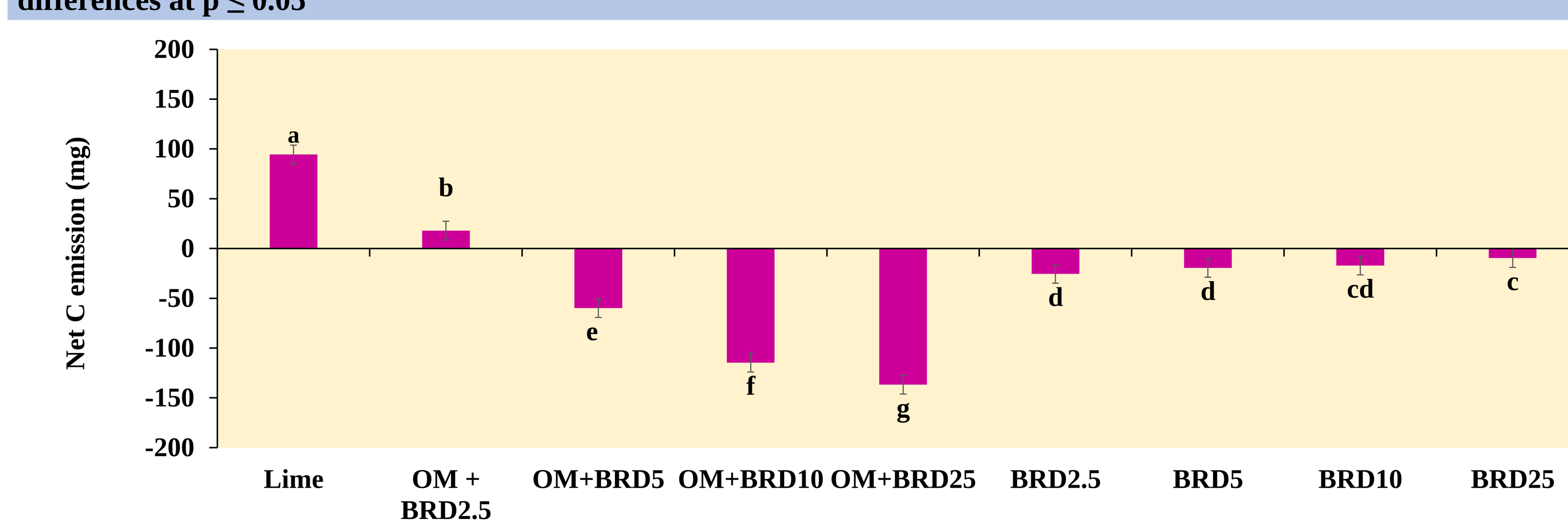

Net cumulative C emission on the 128th day from the inputs showed that the net negative emission was highest in the treatments OM + BRD_{25}, followed by OM + BRD_{10}, and OM + BRD_5 whereas lime and OM + $BRD_{2.5}$ showed net positive emission

Fig. 6. Moving average graph for calculation of the best possible dose of BRD for carbon removal

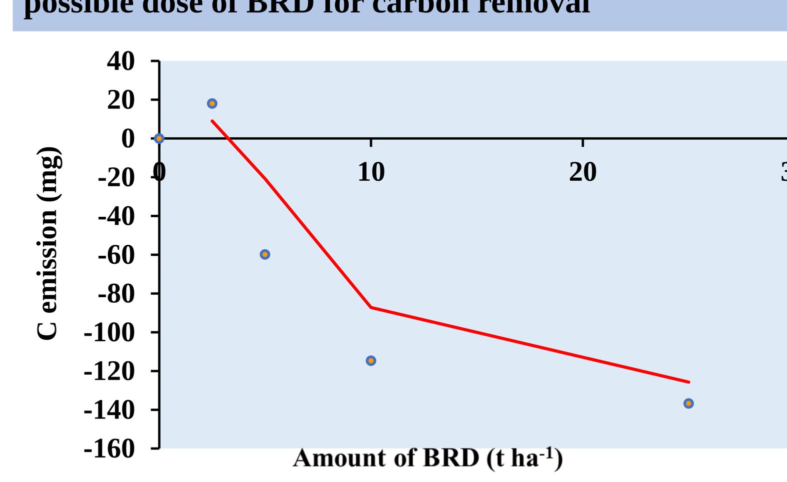

Fig. 7. Second-order polynomial graph for calculation of the best possible dose of BRD

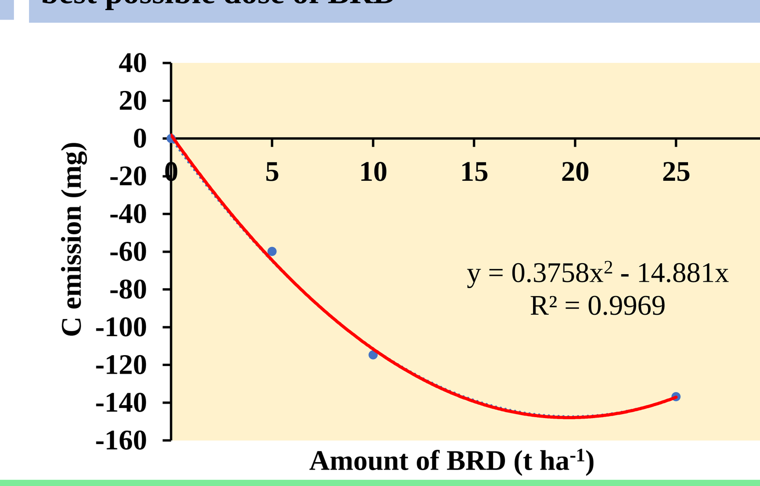

The net C emission was plotted against the BRD doses, and a moving average graph was generated. The break-even point, marked by a change in slope, was identified at 10 t ha^{-1}. To determine suitable BRD doses for farmers' fields, the best-fitted trendline was a second-order polynomial function with an intercept of zero.

The slopes that were found by differentiation were statistically analyzed, and the lowest RMP dose corresponding to the highest negative slope was identified at 8 t ha-1 at 25 °C as the optimum RMP dose for the field trial

Fig. 8. Periodic changes of soil acidity under the application of lime, organic matter, and BRD. Data represent the mean of 3 replicates. Error bar represents the standard error of estimation

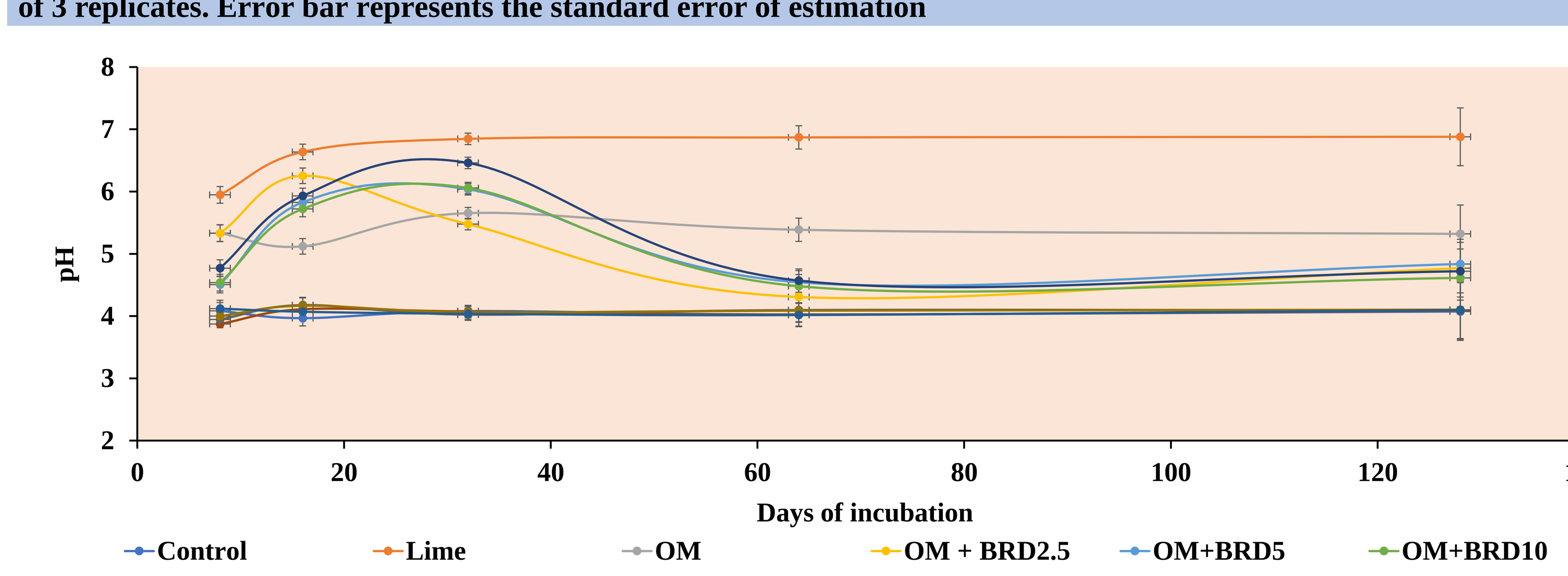

Combined application of BRD and organics ensures a sudden increase in pH of extremely acidic soil within a fortnight after their application

Conclusion

- **The BRD has the potential to capture atmospheric CO_2. Incorporating organic materials enhances BRD dissolution, thereby improving its CO_2 removal efficiency.**
- **The application rate of BRDs might be recommended @ 8 t ha^{-1} along with organics @ 10 t ha^{-1} with a carbon removal potential of 356 Kg ha^{-1}, which, if extrapolated for potential use in pan-India acid soils, results in a carbon removal potential of 0.32 Gt.**
- **The combination of BRDs and organics effectively raises soil pH in highly acidic soils within two weeks. This prevents seed injury and germination delays, positioning it as a carbon-neutral solution for reclaiming acidic soils in India.**

References

- Beerling, D. J., Kantzas, E. P., Lomas, M. R., Wade, P., Eufrasio, R. M., Renforth, P. and Banwart, S. A. (2020) Potential for large-scale CO_2 removal via enhanced rock weathering with croplands. *Nature*, **583**, 242-248.
- Dietzen, C., Harrison, R. and Michelsen-Correa, S. (2018) Effectiveness of enhanced mineral weathering as a carbon sequestration tool and alternative to agricultural lime: an incubation experiment. *International Journal of Greenhouse Gas Control* **74**, 251-258

Use of seaweed extract-based biostimulants for enhancing nutrient use efficiency and grain quality in an Indian acid soil

ABIR DEY, BIJAN KUMAR MONDAL, DEBARUP DAS, MC MEENA and DEEPAK[1]
Indian Agricultural Research Institute, New Delhi, India
[1]Indian Institute of Soil Science, Bhopal, India
Corresponding author e-mail id: abirdey21@gmail.com

Introduction

Rising cost of synthetic fertilizers and environmental concerns over their excessive and unbalanced use drive a global shift towards organic regenerative farming.

In recent times, seaweed extracts have emerged as promising bio-stimulant for crop growth and nutrition.

Integration of seaweed extract-based products (SWEP) with synthetic fertilizers is increasingly vital and being considered as nature positive agricultural practice.

However, their effects on soil physico-chemical properties and plant growth remain poorly understood.

The present study was carried out using a highly acidic soil (pH 3.87) to evaluate the impact of seaweed extract-based *Sagarika* Z++ granules (SG) and *Sagarika* liquid (SL) developed by the Indian Farmers Fertilizer Cooperative (IFFCO), on physio-biochemical activity, nutrient use efficiency and grain quality of wheat grown in a greenhouse pot experiment

Objectives

- To evaluate the impact of seaweed extract-based products on biochemical activities of wheat grown under greenhouse pot experiment
- To study the effects of seaweed extract-based products on yield and grain quality of wheat
- To examine the effects of seaweed extract-based products on nutrient use efficiency of wheat grown in an acid soil

Methodology

Table 1 Details of treatments used for the greenhouse pot study

Treatment codes	Treatment description
Control	Soil
100% NPK	100% NPK
75% NPK	75% NPK
75% NPK + SG(5.33)	75% NPK + seaweed extract-based granular product @ 5.33 mg kg^{-1} soil
75% NPK + SG(10.67)	75% NPK + seaweed extract-based granular product @ 10.67 mg kg^{-1} soil
75% NPK + SG(21.33)	75% NPK + seaweed extract-based granular product @ 21.33 mg kg^{-1} soil
75% NPK + SL(2.5)	75% NPK + seaweed extract-based liquid product spray @ 2.5 ml L^{-1} of water
75% NPK + SL(5)	75% NPK + seaweed extract-based liquid product spray @ 5 ml L^{-1} of water
75% NPK + SL(7.5)	75% NPK + seaweed extract-based liquid product spray @ 7.5 ml L^{-1} of water
75% NPK + SG(10.67) + SL(5)	75% NPK + seaweed extract-based granular product @ 10.67 mg kg^{-1} soil + seaweed extract-based liquid product spray @ 5 ml L^{-1} of water

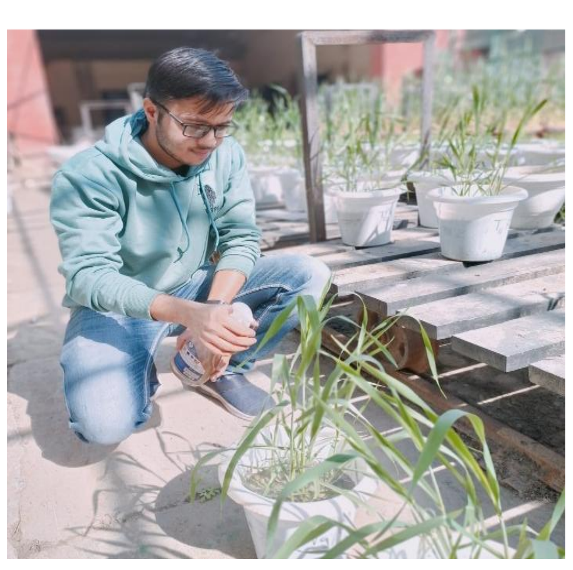

Experimental design: Completely Randomized design, No. of replications: 5, Crop: Wheat, Variety: HD 3086

Table 2 Physico-chemical properties of seaweed extract-based products

Parameters	Seaweed extract-based granular product	Seaweed extract-based liquid product
pH	8.58	6.95
Electrical conductivity (dS m^{-1})	0.082	0.96
Total dissolved solids (%)	_	28.6
Solubility in 0.01M $CaCl_2$ (SG: solvent = 1:100, w/v)		_
In 1 hour	16%	
After 24 hours	28%	
Beyond 24 hours	28%	
Grain size distribution		_
Diameter >2 mm	94.8%	
Diameter 1-2 mm	0.4%	
Diameter <1 mm	0.8%	
Carbon content (%)	5.37	2.1
N content (%)	0.49	0.25
P content (%)	0.028	0.006
K content (%)	0.54	14.2
S content (%)	6.5	1.3
Ca content (%)	26.4	0.16
Mg content (%)	6.7	0.025
Fe content (mg kg^{-1})	1270	138
Zn content (mg kg^{-1})	11400	3.58
Mn content (mg kg^{-1})	6.53	13.8
Cu content (mg kg^{-1})	24.3	1.84
Auxin	42.3	341.7
Gibberellin	39.5	611.6
Cytokinin	28.8	223.3
Glycine betaine	21.4	94.5

Results and discussion

Table 3 Effect of seaweed extract-based biostimulants on different biochemical parameters in wheat flag leaf at ear emergence stage. Data represent the mean of 4 replicates. Within a column, different letters denote significant difference at $p \leq 0.05$

Treatment	Protein content (mg g^{-1} FW)	Non-enzymatic anti-oxidant			Enzymatic anti-oxidant		
		Prolin content (mg g^{-1} FW)	Phenol content (mg g^{-1} FW)	Anti-oxidant activity (%)	SOD (U g^{-1} FW)	Peroxidase (mM TG formed min^{-1} g^{-1} FW)	Catalase (mM of H_2O_2 decomposed min^{-1} g^{-1} FW)
Control	22.5f	0.557a	1.304a	40.2a	1.507e	52.8f	0.031g
100% NPK	23.2ef	0.237e	0.497d	16.6d	1.9ab	76.5d	0.278b
75% NPK	22.9ef	0.382c	0.963b	29.9b	1.623de	62.267e	0.115e
75% NPK + SG(5.33)	24.5cd	0.339d	0.47d	23.8c	1.72cd	91.379c	0.11e
75% NPK + SG(10.67)	23.8de	0.417b	0.477d	17.4d	1.656cd	90.333c	0.107e
75% NPK + SG(21.33)	25.5bc	0.343d	0.459d	19.7cd	1.883ab	105.2ab	0.058f
75% NPK + SL(2.5)	25.3bc	0.249e	0.463d	17.2d	1.77bc	108.767a	0.145d
75% NPK + SL(5)	24.7bcd	0.168f	0.739c	20.0cd	1.872b	103.133b	0.213c
75% NPK + SL(7.5)	25.8ab	0.15f	0.752c	18.83d	1.78bc	101.367b	0.326a
75%NPK+SG(10.67) +SL(5)	26.8a	0.115g	0.459d	19.4d	2.013a	105.833ab	0.344a
LSD (p = 0.05)	1.19	0.018	0.071	4.29	0.137	5.519	0.024

- Nutrient deficiency is a major factor inducing abiotic stress, involving hyperosmotic and ionic imbalances leading to excess production of reactive oxygen species in control and 75%NPK.
- The alleviated levels of non-enzymatic antioxidants *i.e.*, proline and phenol content in the nutrient-deficient treatments *i.e.*, control and 75% NPK indicate towards implementation of nutrient stress.
- Combined application of granular and liquid SWEP in the treatment 75% NPK + SG(10.67) + SL(5) resulted in the maximum production of SOD, peroxidase, and catalase hinting at greater alleviation of oxidative stress
- Synergistic impact of both liquid and granular SWEPs on growth promotion and oxidative stress neutralization might have resulted in the maximum scavenging of ROS under the 75% NPK + SG(10.67) + SL(5)

Table 4 Effect of seaweed extract-based biostimulants on yield and grain quality parameters of wheat. Data represent the mean of 4 replicates. Within a column, different letters denote significant difference at $p \leq 0.05$

Treatments	Grain yield (g/pot)	Straw yield (g/pot)	Harvest Index (%)	Total starch content (%)	Amylose content (%)	Crude protein content (%)
Control	3.33e	5.53e	37.6a	46.87e	10.57f	6.33d
100% NPK	6.2ab	10.4bc	37.4a	64.367bc	25.96abc	9.24a
75% NPK	5.47d	9. 83d	35.7b	60.97d	21.67e	8.14c
75% NPK + SG(5.33)	5.63cd	10.1cd	35.8b	62.63cd	23.433cde	8.62b
75% NPK + SG(10.67)	5.73bcd	10.6abc	35.1b	62.033cd	22.7de	8.55bc
75% NPK + SG(21.33)	5.67cd	10.67ab	34.7b	63.7bc	22.97cde	8.72b
75% NPK + SL(2.5)	5.8bcd	10.47abc	35.6b	66.83a	22.97cde	8.55bc
75% NPK + SL(5)	5.87bcd	10.53abc	35.8b	67.1a	24.87bcd	8.62b
75% NPK + SL(7.5)	6.03bc	10.63ab	36.2ab	65.97ab	26.97ab	8.46bc
75%NPK+SG(10.67) +SL(5)	6.63a	10.97a	37.7a	68.1a	28.82a	8.85ab
LSD (p = 0.05)	0.475	0.53	1.51	2.37	3.15	0.46

- Neutralization of nutrient stress under 75% NPK + SG(10.67) + SL(5) resulted in similar growth and productivity in the former compared with the 100% NPK application.
- The improvements in photosynthetic activity, delayed senescence, and higher enzymatic activities upon foliar application of SWEP resulted in greater formation of carbohydrates. The phytohormones in SWEP promoted mobilization of these photosynthates to the reproductive parts, and enhancing the total starch content of wheat grains, compared with other treatments.
- On the other hand, soil application of SWEP enhances root absorption capacity, and increases the bio-availability of soil nutrients.
- The combined foliar and soil application of SWEP in 75% NPK + SG(10.67) + SL(5) synergistically affected the grain carbohydrate content, registering the highest values of total starch, and amylose content.
- The bio-stimulatory activities of SWEP, along with the efficient use and uptake of N and S promoted the formation of crude protein.

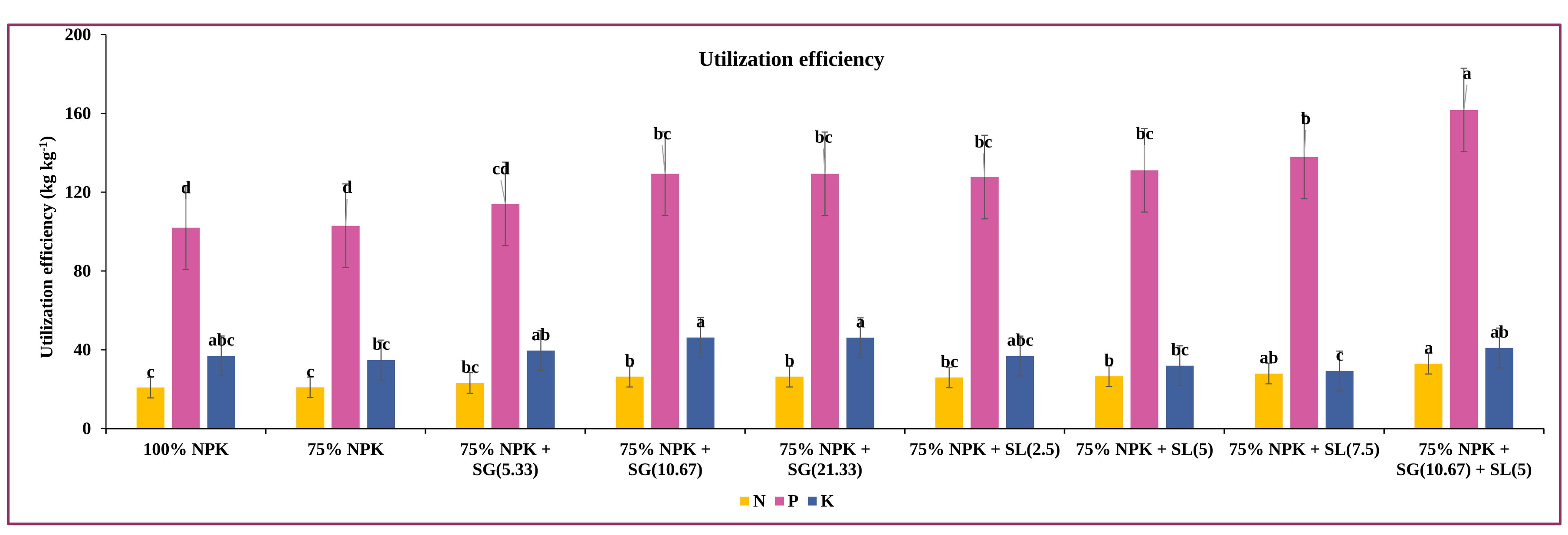

Figure 1: Effect of seaweed extract-based biostimulants on utilization efficiency. Data represent the mean of 4 replicates and error bar represent LSD at 5% level of significance. Different letters denote significant difference at $p \leq 0.05$.

- Application of SWEPs under suboptimal fertilization in an extremely acidic soils resulted in improved soil physicochemical characteristics viz. soil pH, SOC and Available N, P and K and better microbial colonization in the rhizosphere region coupled with higher activities of nutrient cycling enzymes
- As a result of comparable nutrient uptake under 75% NPK + SG(10.67) + SL(5) and 100% NPK, and a lower nutrient application under the former, a higher use efficiency *i.e.*, UE of N and P was registered under the 75% NPK + SG(10.67) + SL(5) compared with the 100% NPK

Conclusions

- Spraying of seaweed extract based liquid biostimulant improved biochemical activities and grain quality of wheat, while application of granular product showed significant positive effects on physico-chemical and microbiological properties of soil.
- Combined application of seaweed extract-based granules @ 10.67 mg/kg soil (equivalent to 25 kg/ha) and 2 sprays of seaweed extract-based liquid biostimulant @ 5 ml/L along with 75% NPK fertilization, improved N and P use efficiencies without any apparent signs of nutrient mining and holds the potential to curtail fertilizer NPK application by 25%.

Future directions

Future research needs to focus on multi-locational field-level studies exploring different dosages of SWEP on crop performance, soil nutrient dynamics and rhizosphere ecosystem under varied settings of climate, soil, and plant types, across the Country

Correspondence E-mail: abirdey21@gmail.com

Agriculture and Agri-Food Canada
Agriculture et Agroalimentaire Canada

Yield projections and expansion opportunities under future climate change for seven major crops grown in Canada using a model ensemble

Ward Smith[1], Brian Grant[1], Qi Jing[1], Budong Qian[1], Guillaume Jégo[2] and Marianne Crépeau[2]

[1]Agriculture and Agri-Food Canada, Science and Technology Branch, Ottawa Research and Development Centre, Ottawa, Canada

[2]Agriculture and Agri-Food Canada, Science and Technology Branch, Quebec Research and Development Centre, Quebec City, Canada

Introduction

As global temperatures rise, understanding and managing the impacts of climate change on crop production in Canada is key towards ensuring the long-term sustainability of the sector. A warming climate, particularly in regions like Canada, has already led to increases in available crop heat units and longer frost-free periods, however in the future, some agricultural regions may experience higher incidences of drought, increased crop heat stresses and excessive water exposure.

Materials & Methods

The DSSAT, STICS and DNDC models estimated changes in yields for seven major crop types (maize, wheat, canola, soybean, barley, potato, and forage alfalfa) across Canada for the period 1981 to 2100, considering 51 regions where crops are currently grown and possible areas of expansion. The models were previously verified for simulating crop growth and development within several AgMIP initiatives and using local Canadian sites and cultivars. Simulations were performed using climate scenarios based on five GCMs under three shared socioeconomic pathways (SSP1-2.6, SSP3-7.0, SSP5-8.5) from phase 3b of the Inter-Sectoral Impact Model Intercomparison Project. Simulated planting date was adjusted each year based on temperature and soil moisture status. Results are presented for the Baseline (2006-2015), 2030 mean (2026-2035), 2050 mean (2046-2055) and 2070 mean (2066-2075).

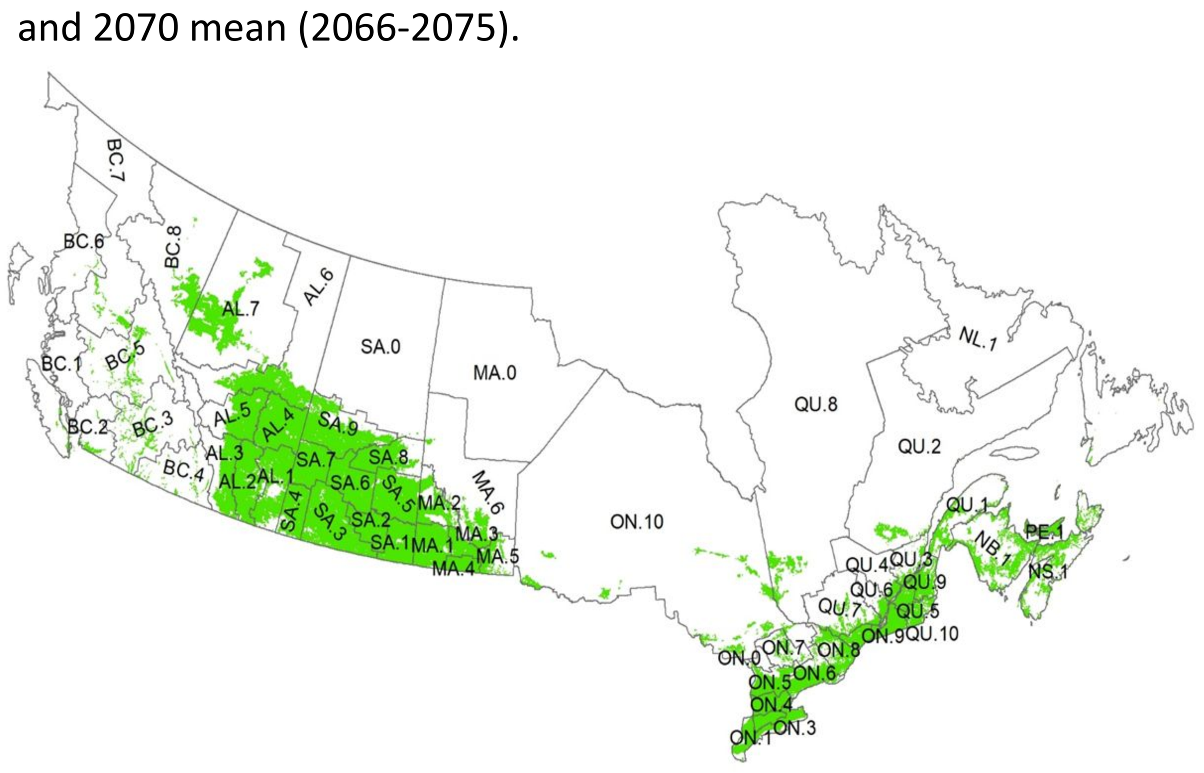

Figure 1. Canadian Regional Agricultural Model (CRAM) economic model regions simulated using DSSAT, STICS and DNDC for 5 GCMs and 3 climate scenarios. The green areas indicate current agricultural production.

Climate projections from the five GCMs showed greater crop heat units (CHU) across Canada, longer frost-free periods, resulting in longer growing seasons. CHU increased drastically across the country which may allow for later maturing cultivars and more forage harvests each year. Under the SSP370 scenario the frost-free period increased from 128 to 163 days in the semi-arid prairies and from 149 to 190 days in southern Ontario and Quebec by 2070. Precipitation is generally projected to remain relatively stable across Canada with potentially greater soil moisture deficit in the semi-arid prairies, which may be offset through CO_2 fertilization which decreases stomatal conductance. Annual crop failure due to cold stress and frost damage is projected to decrease for all crops.

Table 1 Regional average changes in growing season precipitation, crop heat units, frost free days and crop failure rate under SSP370

	Time period	Humid East < 47° lat	Humid East > 47° lat	Semi-arid West	Sub-humid West < 51°	Sub-humid West > 51°
Growing season precipitation (mm)	Baseline	479	478	274	346	346
	2030	472 (-1.4%)	490 (+2.4%)	272 (-0.7%)	334 (-3.6%)	351 (+1.6%)
	2050	473 (-1.3%)	491 (+2.7%)	277 (+0.8%)	340 (-2.0%)	355 (+2.5%)
	2070	482 (+0.7%)	498 (+4.2%)	264 (-3.6%)	331 (-4.3%)	345 (-0.3%)
Crop heat units	Baseline	2549	1709	2200	2205	1304
	2030	3154 (+24%)	2264 (+32%)	2751 (+25%)	2823 (+28%)	1899 (+46%)
	2050	3520 (+38%)	2608 (+53%)	3069 (+39%)	3145 (+43%)	2277 (+75%)
	2070	3874 (+52%)	2956 (+73%)	3369 (+53%)	3474 (+58%)	2668 (+105%)
Frost free days	Baseline	149	112	128	139	119
	2030	169 (+12%)	131 (+17)	142 (+11)	155 (+11)	138 (+16)
	2050	178 (+20%)	143 (+28)	152 (+19)	165 (+19)	150 (+26)
	2070	190 (+28%)	155 (+39)	163 (+27)	177 (+28)	163 (+37)
Annual failure percentage (e.g., soybeans)	Baseline	3	16	54	11	48
	2030	0	4	45	9	25
	2050	0	1	39	8	18
	2070	1	0	39	9	15

Results & Discussion

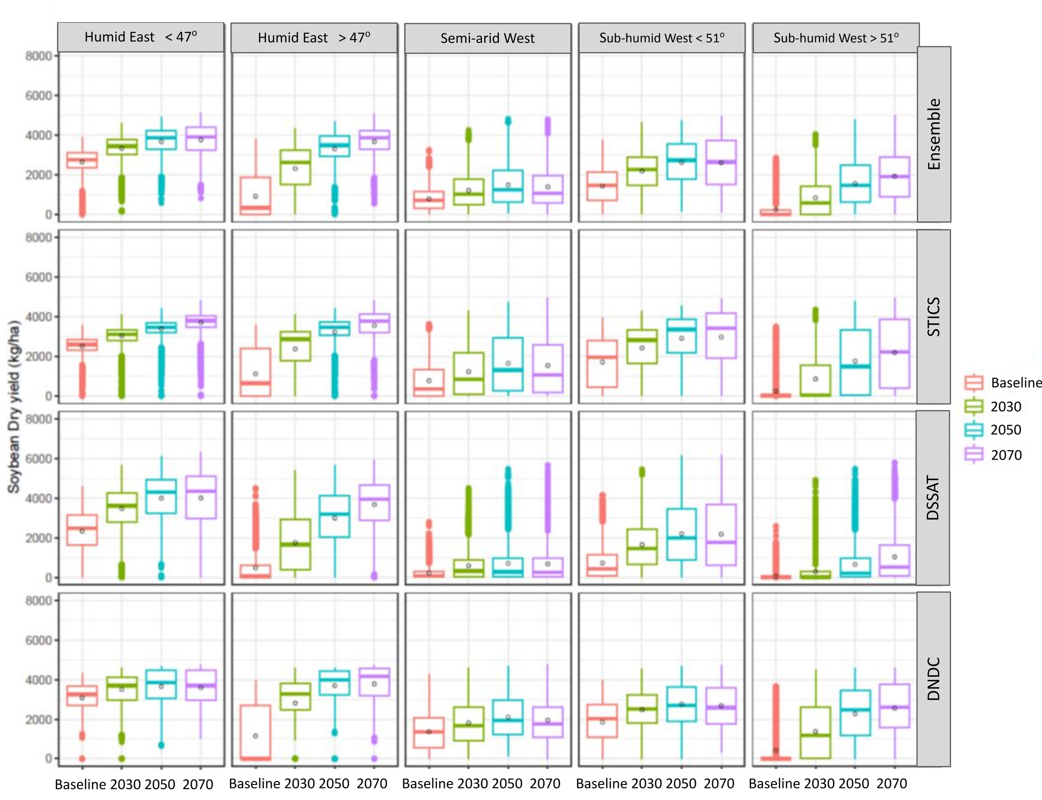

Figure 2. Projected rainfed soybean yields for each model and the model ensemble under SSP370

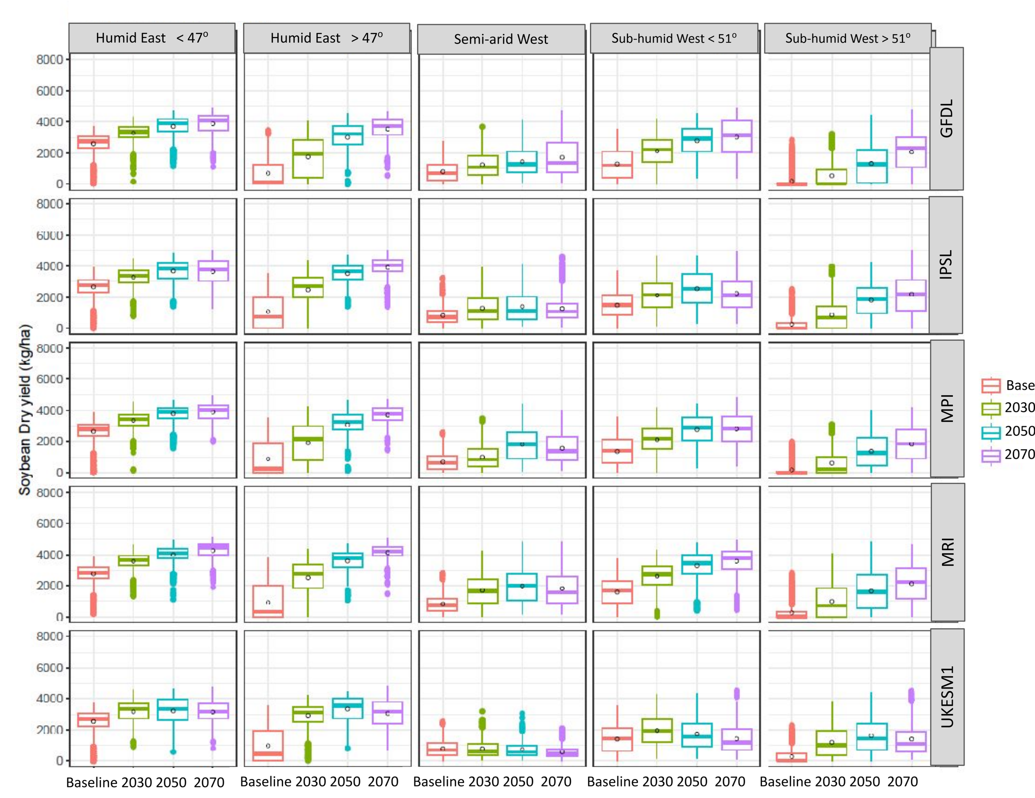

Figure 3. Projected rainfed soybean yields for each GCM under SSP370

When evaluated independently, the three crop models consistently projected an increase in soybean yields across Canada, with the most gain occurring by 2050. A similar trend was observed for other crop types. Likewise, four of the five GCM yield projections agreed, whereas UKESM1 indicated yield increases only until 2050.

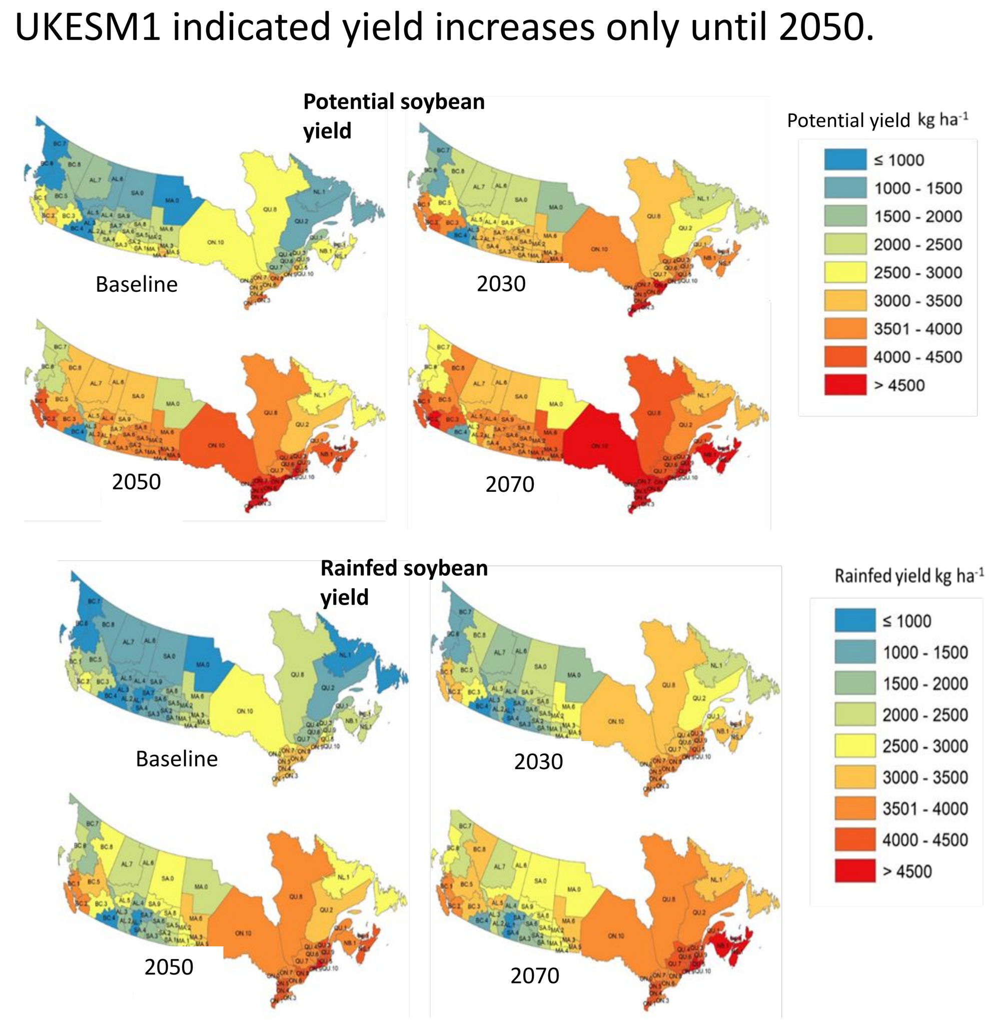

Figure 4 Potential and rainfed soybean yields within CRAM regions

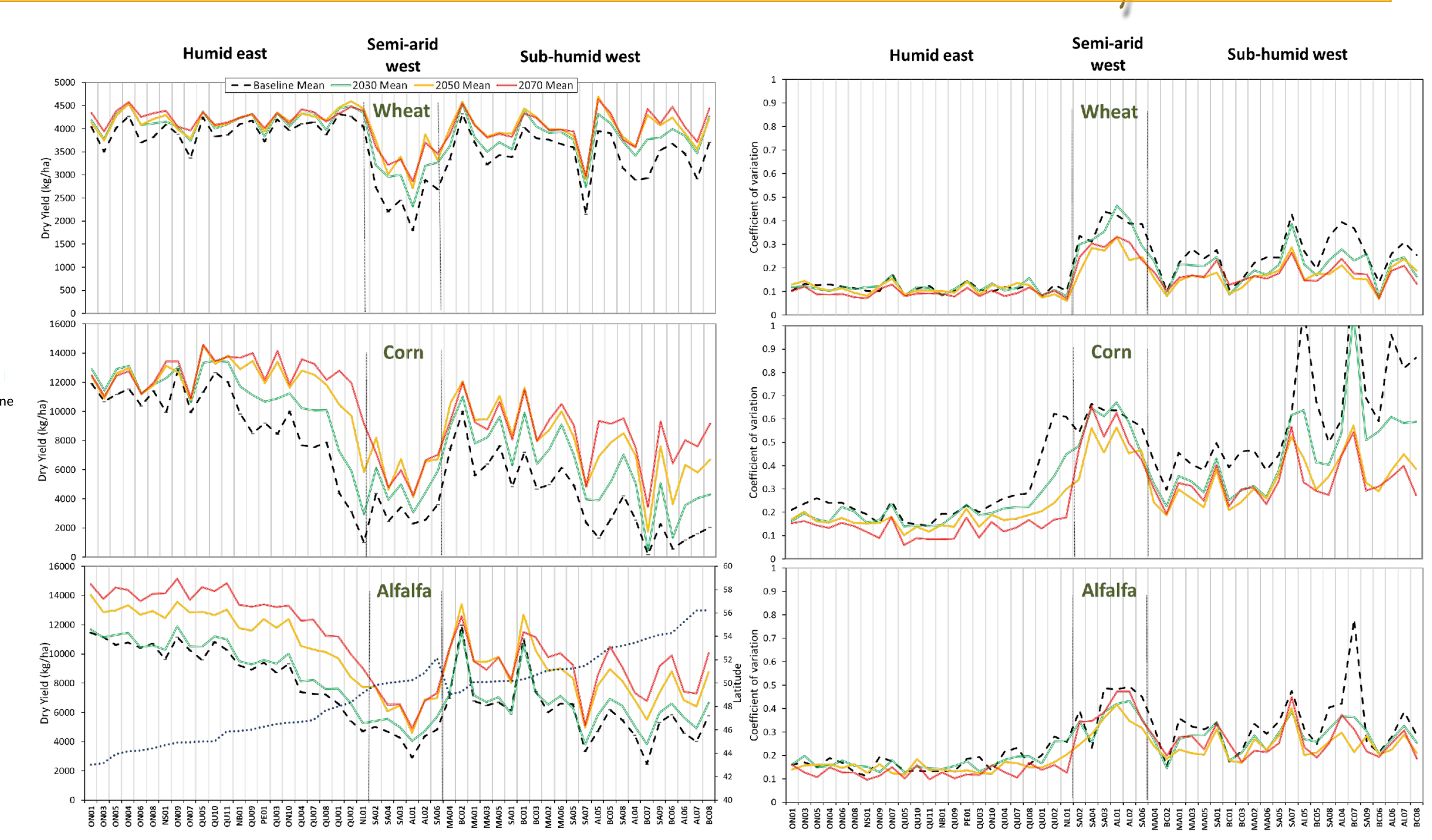

Figure 5. Projected rainfed yields and coefficient of variation for yields across Canada for wheat, corn and alfalfa using DSSAT, STICS and DNDC under SSP370

Future climate conditions, characterized by warmer temperatures, longer growing seasons, and enhanced CO_2 levels, are projected to generally increase crop yields across most regions in Canada. Wheat, canola, alfalfa, and barley yields could rise by 5–15% under these conditions. While rainfed agriculture in the semi-arid prairies will continue to face constraints, the three crop models coupled with global climate model projections from the IPCC's 6th assessment indicate no significant increase in yield volatility across the country. The combined effects of higher CO_2 levels and reduced cold damage are expected to outweigh the negative impacts of increased heat stress and greater potential evapotranspiration. Among the investigated crops, soybean, alfalfa, and maize are projected to benefit the most in humid and subhumid regions, with yield increases of approximately 20–30% by the 2050s in areas where they are currently grown. By the 2030s, some crops, including soybeans, maize, barley, wheat, and canola, may expand northward. However, specific growth traits, such as photoperiod requirements, could limit their expansion potential.

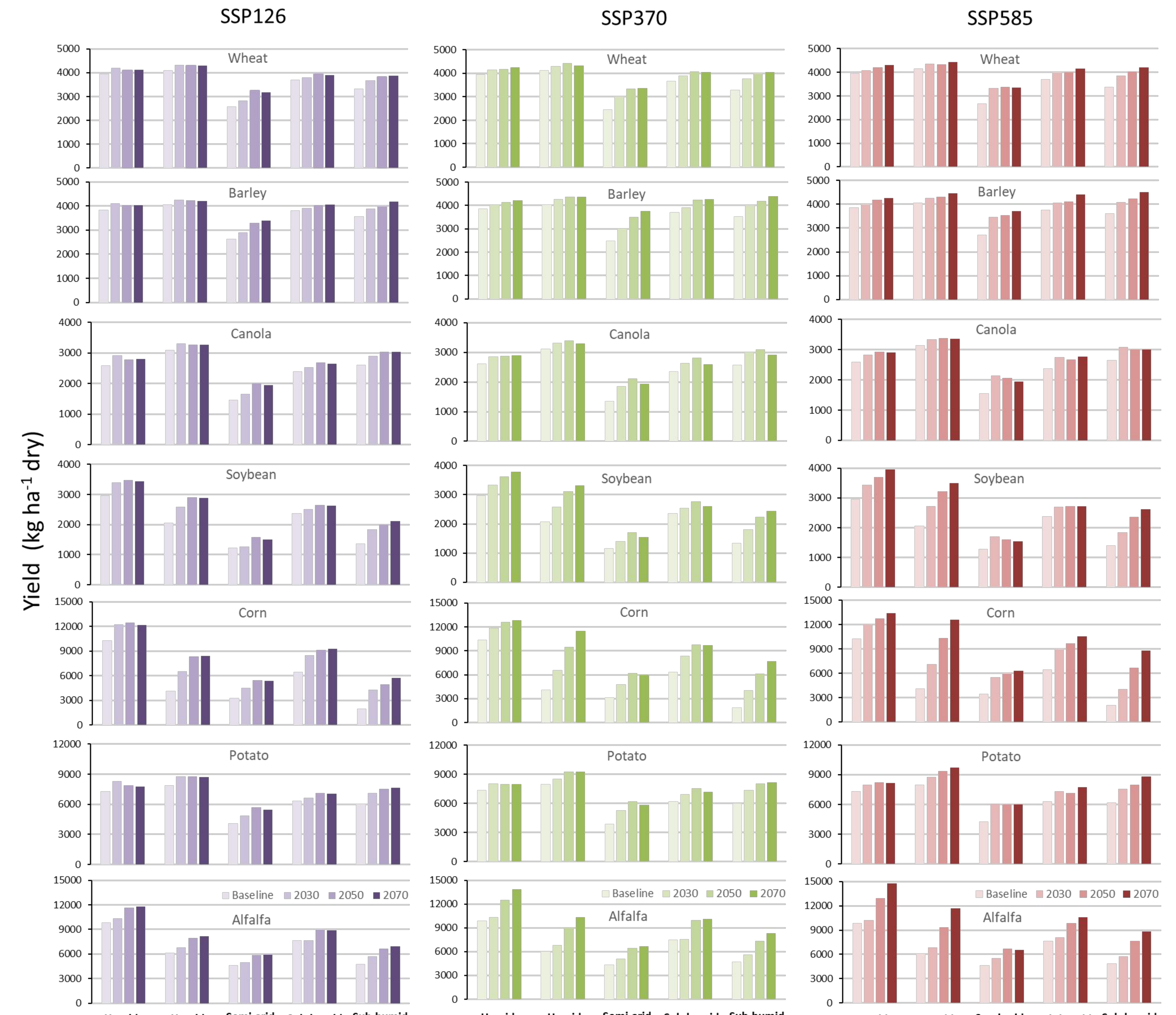

Figure 6. Projected yields within five regions for seven crop types across Canada

Conclusions

A future warmer climate with longer growing seasons is expected to increase yields for major crops across much of Canada. Crop water stress in the semi-arid prairies will likely continue to constrain yields, though overall yield volatility is projected to remain stable. Some crops may expand northward into regions where they are not currently grown, but this expansion may be restricted to early-maturity cultivars and by soil quality. While changes in abiotic stresses indicate future climate change may enhance agricultural production, these benefits must be weighed against potential challenges such as extreme weather events, emerging diseases and pests, and broader environmental and economic consequences, factors that were not considered in this study.

AgMIP10 Responding to Climate Change Urgency

March 31-April 4, 2025
CIMMYT, El Batan, Mexico

McGill FACULTY OF Agricultural and Environmental Sciences

Agriculture and Agri-Food Canada | Agriculture et Agroalimentaire Canada

Advancing the Denitrification and Decomposition Model for Simulating Carbon Decomposition and Carbon dioxide Emissions from Biosolids and Manure Amended Cropland

Ruth Sitienei[a,b], Zhiming Qi[a*], Brian Grant[b], Okenna Obi-Njoku[c], Andrew Vanderzaag[b], Michael Yongha Boh[a], O. Grant Clark[a], Gordon Price[d], Chandra Madramootoo[a], Tiequan Zhang[e], and Ward Smith[b*]

[a]Department of Bioresource Engineering, McGill University, 21111 Lakeshore Road, Ste-Anne-de-Bellevue, QC, Canada, H9X 3V9 [b]Ottawa Research and Development Centre, Agriculture and Agri-Food Canada, 960 Carling Ave, Ottawa, Ontario, K1A 0C6, Canada

[c]Pollutant Inventories and Reporting Division, Environment and Climate Change Canada, 351 Boulevard Saint-Joseph, Gatineau, Quebec J8Y 3Z5, Canada. [d]Department of Engineering, Faculty of Agriculture, Dalhousie University, PO Box 550, Truro B2N 5E3, NS, Canada

[e]Harrow Research and Development Centre, Agriculture and Agri-Food Canada, 2585 County Road 20 Harrow, ON N0R 1G0 Canada

Introduction

- Organic amendments including municipal biosolids, composts, digestates and land-applied manure are increasingly utilized as sustainable options for nutrient and resource reuse.
- Land-applied manures and biosolids involve complex interdependent biogeochemical processes.
- DNDCv.CAN previously showed deficiencies in simulating soil CO_2 emissions from applied municipal biosolids and solid applied cattle manures.

Materials & Methods

(a) Locations of the three field experiments in Truro and Montreal from Google Maps; (b) Bio-Environmental Engineering Complex in Bible Hill, Truro, NS, Canada, Emile Lods Agronomy Research Centre; (c) Montreal, QC, Canada; (d) Eugene F. Whelan Research Farm near South Woodslee, Ontario, Canada

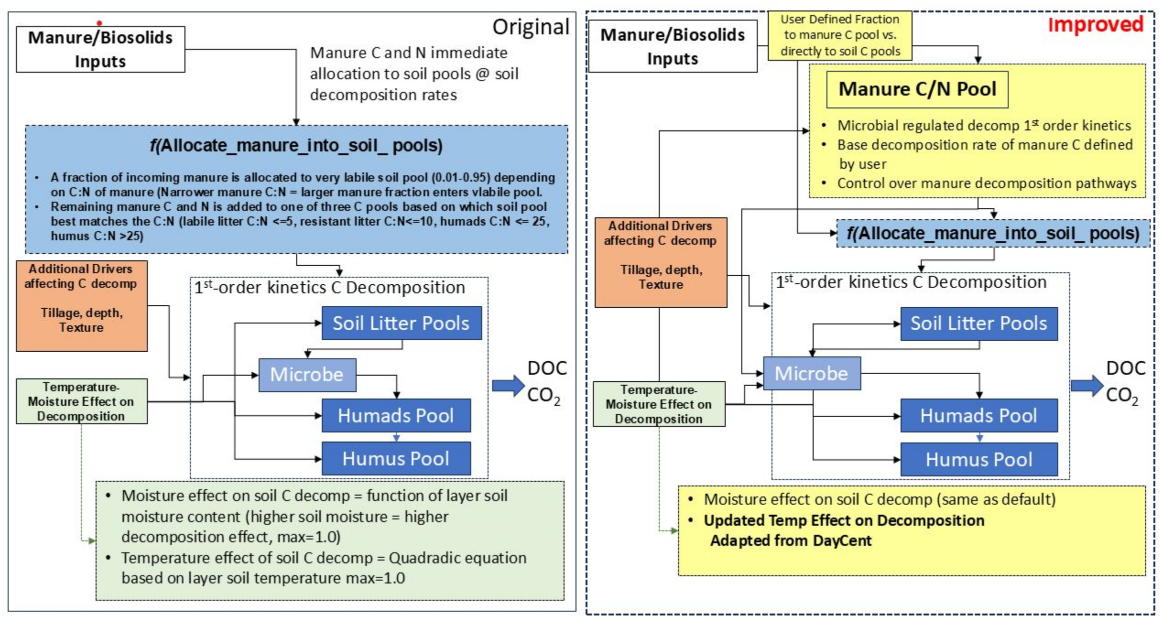

Figure 1. New Manure Pool Dynamics Schematic for Improved DNDC

The C decomposition module of the model was revised by separating the organic C amendments into a separate C pool outside of the SOC pools. This new manure C pool adopts the same first order decomposition concepts that define for the default soil C pools except the base decomposition rates and pathway can now be defined by user inputs. The users can directly control the decomposition dynamics of amendments beyond merely adjusting their C:N ratio characteristics while allocating decomposed C from manure and biosolids into labile and resistant fractions while maintaining the default simulation option. The user-defined fraction of resistant manure C helps reduce associated CO_2 emissions from slower-decomposing biosolid C additions. This is achieved by allowing biosolid C to decompose directly into the microbial pool, bypassing the model's default stepwise decomposition pathways, which would otherwise route manure C through litter fractions before entering the microbial pool and eventually transitioning to the more stable humads and humus pools. This flexibility enhances the model's ability to simulate the decomposition dynamics and CO_2 emissions evolution of biosolid additions over seasonal and annual timescales.

Results & Discussion

Soil temperature

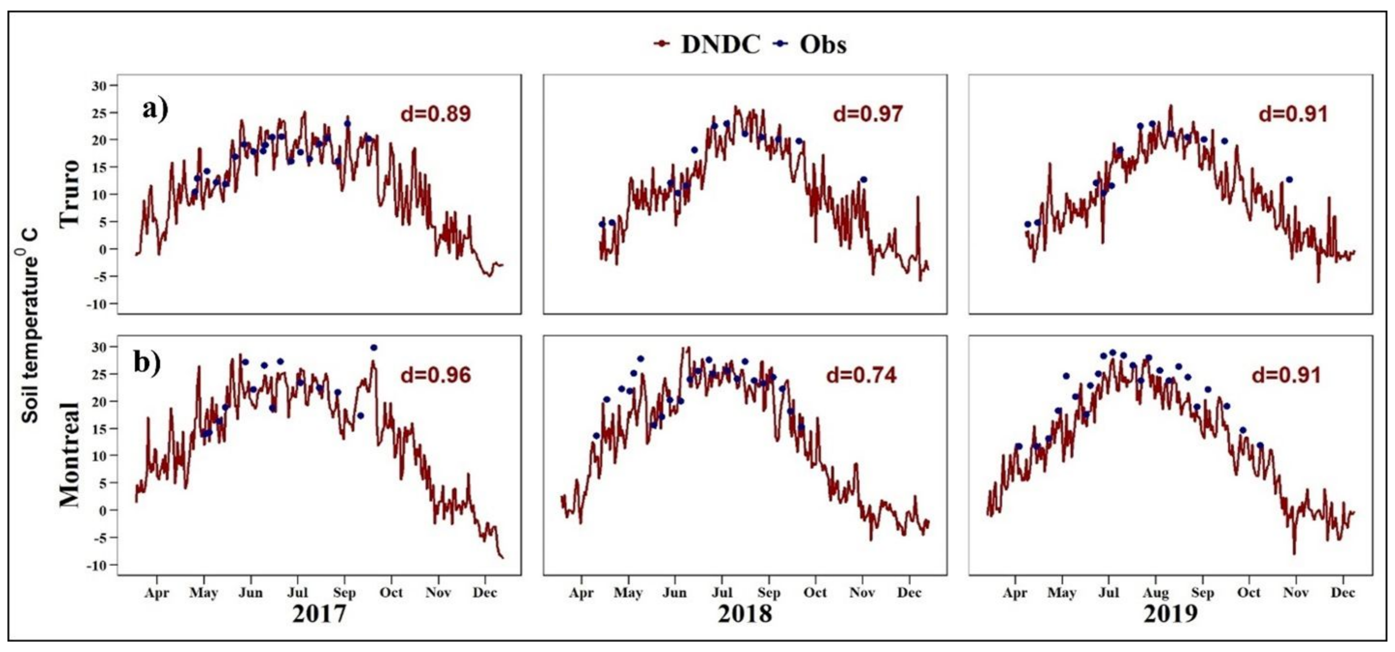

Figure 2. Comparison of DNDC simulated and measured soil temperature in Montreal & Truro

Crop yields

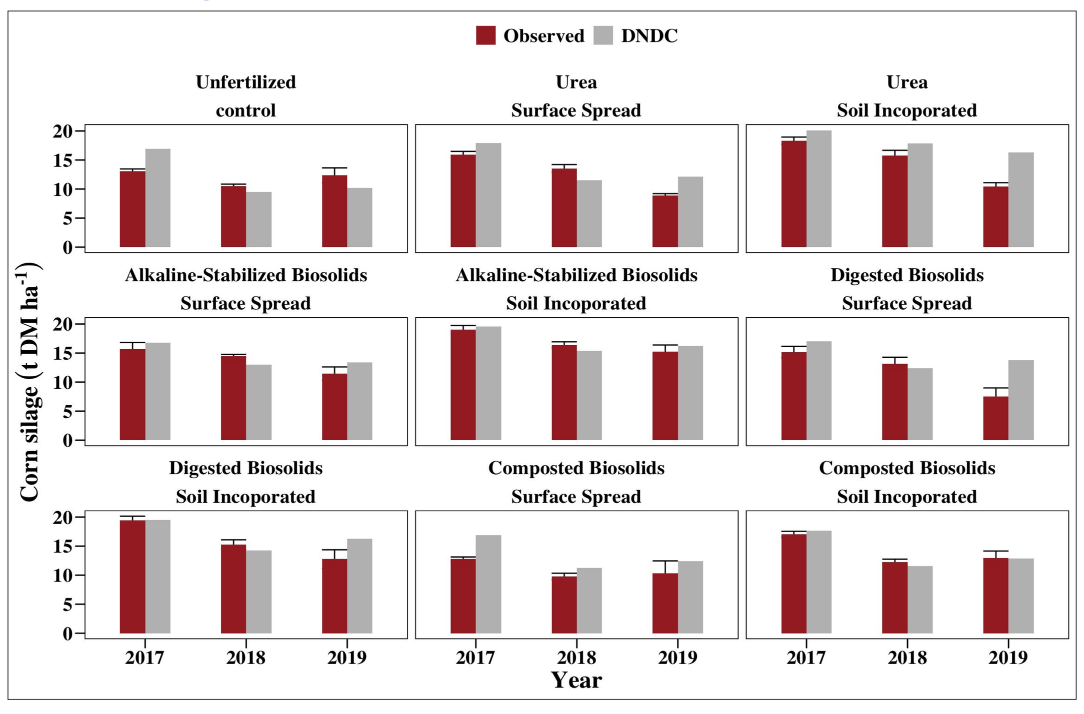

Figure 3. Comparison of DNDC modeled and measured stover yield (dry basis) of silage corn across 2017-2019 at Truro, NS.

Daily carbon dioxide emissions

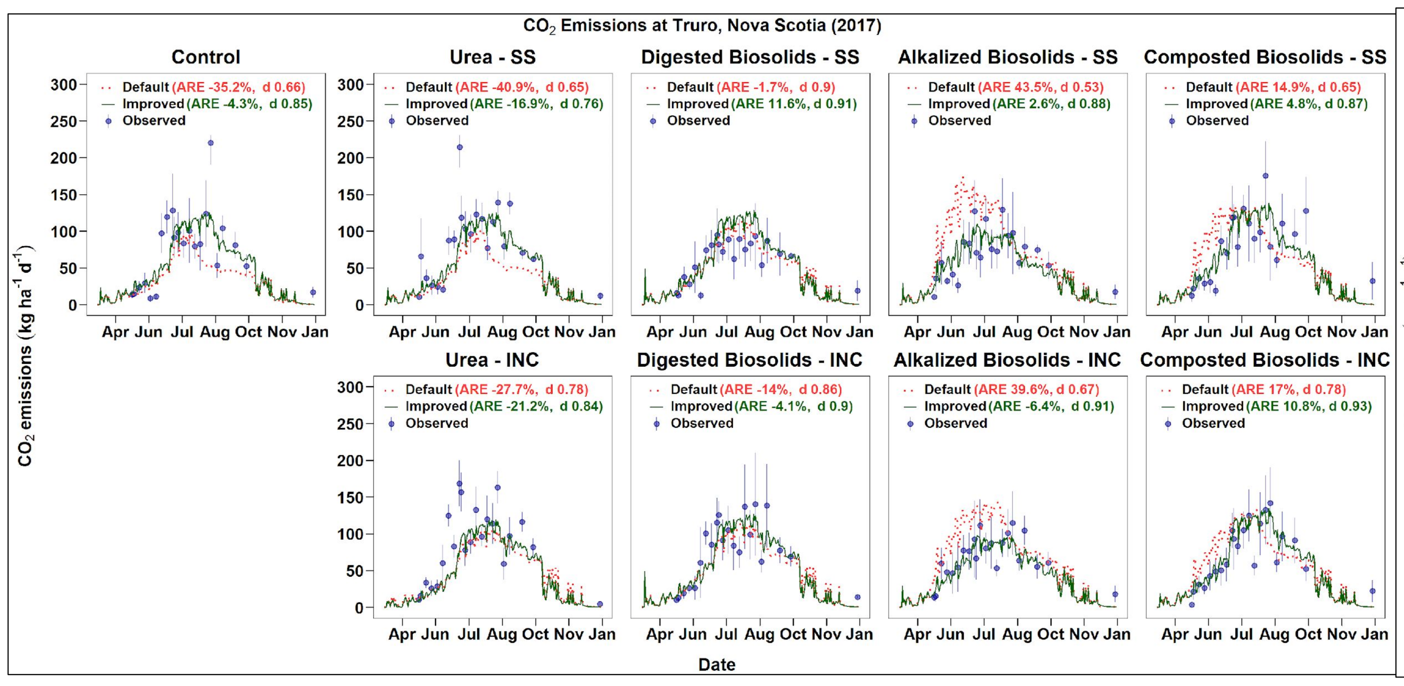

Figure 4. DNDC performance in simulating CO_2 emissions from biosolids at Truro, Nova Scotia, 2017

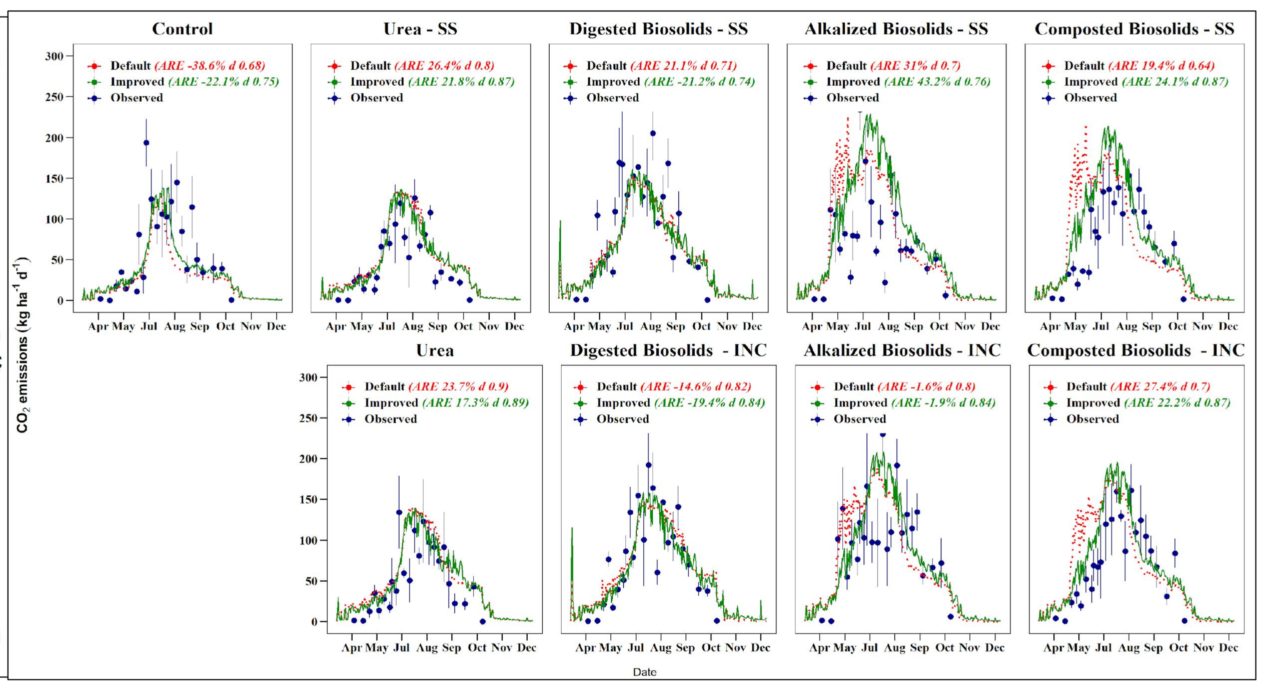

Figure 5. DNDC performance in simulating CO_2 emissions from biosolids at Montreal, Quebec, 2019

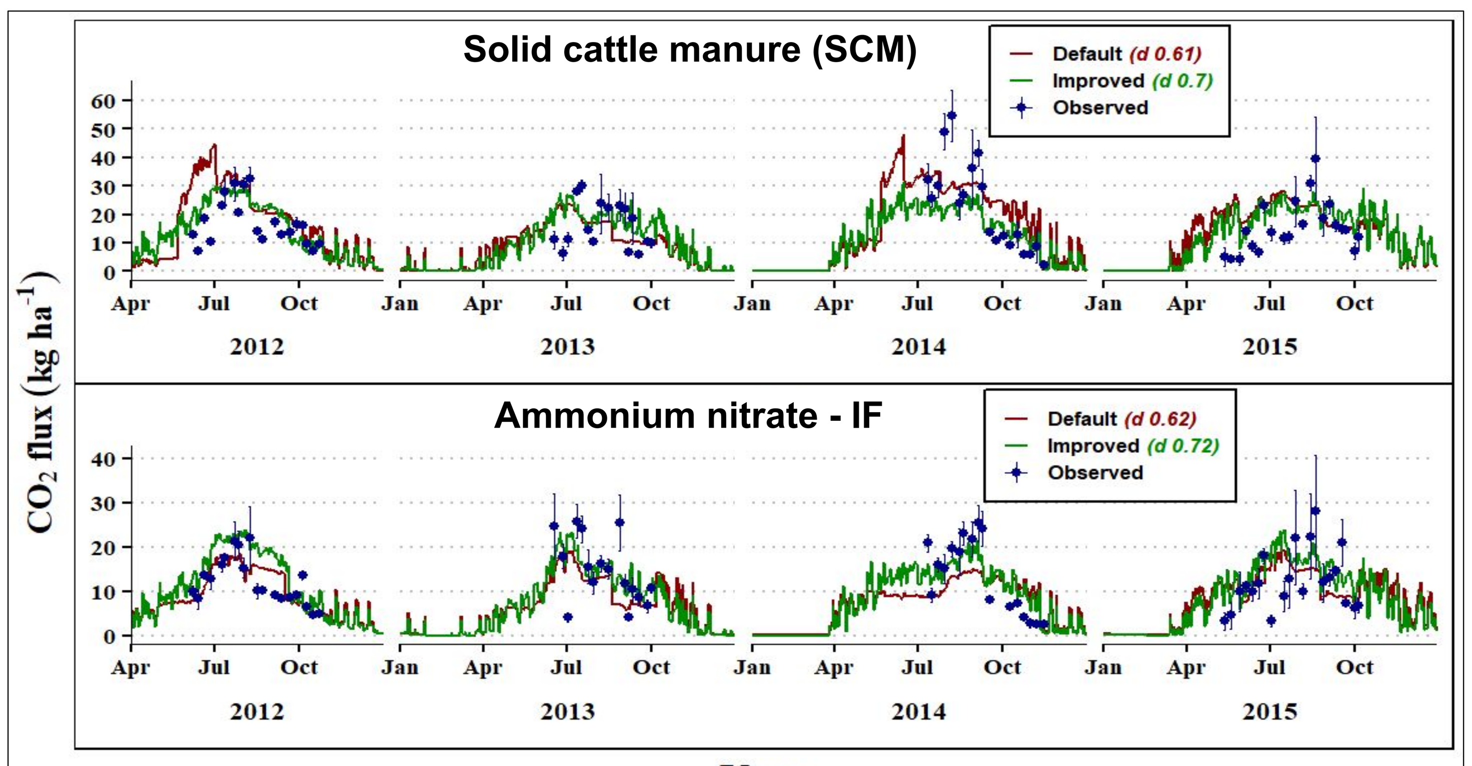

Figure 6. DNDC performance in simulating CO_2 emissions from biosolids at Harrow, Ontario, 2012 - 2015

For *d*-index:	
≥ 0.9	Excellent
0.8 – 0.9	Good
0.7 – 0.8	Fair
≤ 0.7	Poor

Table 1: Statistical performance of models for simulating daily CO_2 emissions

		Calibration (Surface spread treatments)						Validation (Soil incorporated treatments) + Control					
Location	Treatment	ARE%		RMSE (kg C ha^{-1}d^{-1})		d		ARE%		RMSE (kg C ha^{-1}d^{-1})		d	
		Default	Revised	Default	Revised	Default	Revised	Default	Revised	Default	Revised	Default	Revised
Truro	Control							-46.36	-11.07	54.8	28.87	0.67	0.87
	Urea	-41.93	-10.94	42.9	31.37	0.71	0.84	-15.43	-5.37	28.78	25.68	0.86	0.89
	Digested biosolids	-15.92	1.62	32.2	19.99	0.88	0.93	-13.31	2.73	30.87	23.28	0.88	0.92
	Alkalized biosolids	20.54	-2.17	35.59	24.25	0.74	0.87	21.21	5.61	48.63	29.52	0.68	0.78
	Composted biosolids	9.94	5.84	59.49	31.05	0.69	0.88	-5.33	-8.18	57.26	33.02	0.80	0.89
Montreal	Control							-31.46	-14.7	33.68	30.86	0.68	0.77
	Urea	16.54	8.54	23.14	21.88	0.88	0.89	31.33	19.93	22.44	19.71	0.9	0.92
	Digested biosolids	-9.59	-8.09	40.18	39.22	0.81	0.82	-10.75	-12.68	34.94	33.79	0.85	0.87
	Alkalized biosolids	21.99	32.5	53.2	49.69	0.69	0.75	11.88	12.99	43.17	40.87	0.76	0.79
	Composted biosolids	4.44	8.8	60.09	41.51	0.61	0.81	4.14	2.13	49.80	35.67	0.68	0.84
Harrow	Manure + Inorganic fertilizer							-0.65	22.15	10.49	9.43	0.61	0.70
	Inorganic fertilizer	-11.93	12.28	6.16	5.65	0.62	0.72						

Key Findings

- DNDCv.CAN was able to simulate the daily trends in soil temperature and soil water across the three sites.
- The model exhibited reasonable performance for simulating corn stover yields at Truro and Montreal and corn at Harrow (rRMSE 4.1 - 30.1%).
- The improved model better simulated decomposition of organic amendments and CO_2 emissions at Montreal and Truro sites.
- Improvements were apparent across all treatments in both the calibration and validation stages across all the sites (Table 1).
- There was marginal improvements over the default version for simulating CO_2 fluxes from manure at Harrow.
- The performance was greatly improved over a previous version of DNDC published in Jiang et al. 2020 - where d values were 0.48 and 0.58 for IF and SCM, respectively.

Conclusions

- **The revised DNDC model better simulated the magnitude and trends in measured CO_2 fluxes across all experimental sites, including the early season fluxes shown by the observations.**
- **The inclusion of a separate manure pool with user specified decomposition rates and pathways, along with improved temperature effects on SOC decomposition enabled the model to differentiate the organic biosolid types, significantly improving CO_2 trend simulations.**
- **Model performance statistics, RMSE and d, were improved for all treatments.**
- **Overall, this study provides valuable insights into sustainable agricultural practices aimed at optimizing yields while mitigating environmental impacts.**
- **The validated DNDCv.CAN code will be shared with Canadian research institutions and globally via GitHub.**

References

1. Environment and Climate Change Canada. (2023). Environment and Climate Change Canada National Inventory Report 1990–2019: Greenhouse Gas Sources and Sinks in Canada http://www.publications.gc.ca/site/eng/9.506002/publication.html
2. Jiang, Q., Qi, Z., Madramootoo, C. A., Smith, W., Abbasi, N. A., & Zhang, T. Q. (2020). Comparison of Rzwqm2 and Dndc Models to Simulate Greenhouse Gas Emissions under Combined Inorganic/Organic Fertilization in A Subsurface-Drained Field. *Transactions of the ASABE*, *63*(4), 771–787.
3. Obi-Njoku, O., Boh, M. Y., Smith, W., Grant, B., Price, G. W., Hussain, N., Whalen, J. K., & Clark, O. G. (2022). Greenhouse gas emissions following biosolids application to farmland: Estimates from the DeNitrification and DeComposition model. *Science of the Total Environment*, *823*, 153695. https://doi.org/10.1016/j.scitotenv.2022.153695.
4. Sitienei, R., Qi, Z., Grant, B., Obi-njoku, O., Vanderzaag, A., Yongha, M., Clark, O. G., Price, G., Madramootoo, C., Zhang, T., & Smith, W. (2025). A new framework for simulating C decomposition and emissions from land applied biosolids and manures using the denitrification and decomposition model. *Science of the Total Environment*. https://doi.org/10.1016/j.scitotenv.2025.178913.

AgMIP10 Responding to Climate Change Urgency

March 31-April 4, 2025
CIMMYT, El Batan, Mexico

Agronomic strategies to mitigate the yellow berry character in durum wheat in the face of input and water scarcity

Pilar Espitia-Hernández [1]*, José L. Velasco López[1], Norma A. Ruíz Torres[1], Xochitl Ruelas Chacón[2].

[1]Plant Breeding Department, [2]Food Science and Technology Department, Antonio Narro Autonomous Agrarian University, Buenavista, Saltillo, Coahuila. *Email: pilar.espitia1@gmail.com

INTRODUCTION

Durum wheat (*Triticum turgidum* L. var. *durum*) is the tenth most cultivated cereal worldwide and plays a fundamental role in the human diet [**1**]. In Mexico, due to the high costs of nitrogen fertilizers and frequent water shortages for irrigation, the quality of the durum wheat grain is affected due to the yellow berry (YB) character, related to the decrease in grain protein. YB is considered a global problem, with nitrogen shortage being the main cause [**2**].

OBJECTIVE

To evaluate the effects of different irrigation and fertilization regimes to minimize yellow berry (YB) content and maximize grain yield and physical quality of durum wheat under field conditions in Mexico.

MATERIALS AND METHODS

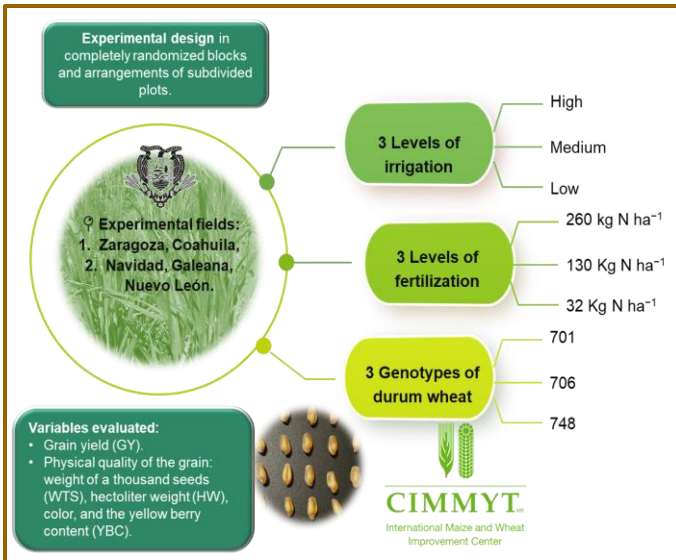

RESULTS AND DISCUSSION

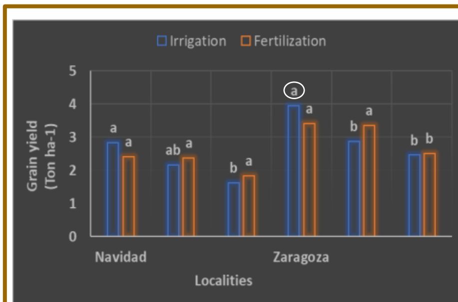

Zaragoza:GY was influenced by irrigation and fertilization factors. GY was positively correlated with TSW (r = 0.76) and HW (r = 0.84) ($p < 0.05$).

Fig. 1. Grain yield (GY) of three wheat genotypes in two locations with different levels of irrigation and fertilization .

Table 1. Comparison of grain physical quality in durum wheat genotypes under different irrigation and fertilization conditions at two locations.

	Genotype	Yellowness (b value)	TSW (g)	HW (kg hl^{-1})	YB Content (%)
Zaragoza	701	22.76 b	41.69 b	76.32 ab	0.86 c
	706	22.49 b	46.73 a	76.55 a	1.72 a
	748	24.39 a	36.63 c	75.94 b	1.27 b
Navidad	701	22.37 b	42.88 b	76.67 a	2.83 b
	706	22.59 ab	46.48 a	77.07 a	1.73 c
	748	23.45 a	37.86 c	75.45 b	4.03 a

Different letters indicate significant differences according to Tukey´s multiple comparison test ($p < 0.05$)

The physical quality variables of both locations were influenced by the effect of the three factors and their interactions.

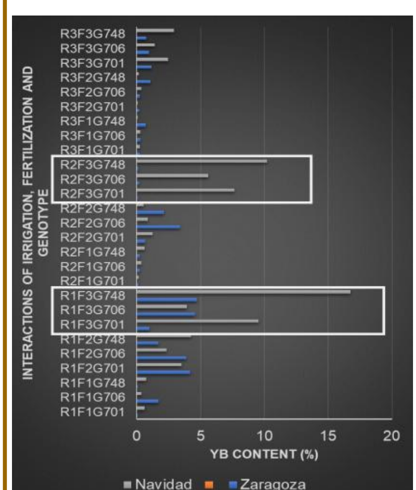

The highest observed value of YB was 16.77% in the locality of **Navidad**. Nitrogen deficiency in the soils of some regions of Mexico, along with drought, reduces wheat yield. Furthermore, low nitrogen fertilization, the use of susceptible varieties, and increased irrigation have been reported to favor the presence of YB in durum wheat [3].

Fig. 2. Yellow berry (YB) content of three wheat genotypes at two locations with different irrigation and fertilization levels.

Navidad: YB was positively correlated with yellowing (r = 0.77) and negatively correlated with TSW (r = -0.99) and HW (r = -0.97). Validated by Pearson's correlation coefficient ($p \leq 0.05$).

CONCLUSIONS

Irrigation and fertilization significantly influence the yield and physical quality of wheat grain, including YB. This study highlights the need to identify genotypes and optimize sustainable agronomic management practices that reduce YB content and improve wheat yield and quality, benefiting farmers and society.

REFERENCES

[**1**] Wan, W., Li, L., Diao, M., Lv, Z., Li, W., Wang, J., Li, Z., Jiang, G., Wang, X., Jiang, D., 2023. Border effects enhance lodging resistance of spring wheat in narrowing-row-space enlarged-lateral-space drip irrigation patterns. [**2**] Ramírez-Wong, B., Rodríguez-Félix, F., Torres-Chávez, P.I., Medina-Rodríguez, C.L., Matus-Barba, E.A., Ledesma-Osuna, A.I., 2014. Effects of nitrogen and irrigation on gluten protein composition and their relationship to "yellow berry" disorder in wheat (*Triticum aestivum*). [**3**] Rodríguez-Félix, F., Ramirez-Wong, B., Torres-Chávez, P. I., Álvarez-Avilés, A., Moreno-Salazar, S., Renteria-Martinez, M. E., & Bello-Perez, L. A. (2014). Yellow berry, protein and agronomic characteristics in bread wheat under different conditions of nitrogen and irrigation in northwest Mexico.